

# UC San Diego

## UC San Diego Previously Published Works

### Title

Compression of Unsaturated Clay under High Stresses

### Permalink

<https://escholarship.org/uc/item/2xk3c4w4>

### Journal

Journal of Geotechnical and Geoenvironmental Engineering, 143(7)

### ISSN

1090-0241

### Authors

Mun, Woongju  
McCartney, John S

### Publication Date

2017-07-01

### DOI

10.1061/(asce)gt.1943-5606.0001668

Peer reviewed

# 1            **COMPRESSION OF UNSATURATED CLAY UNDER HIGH STRESSES**

2            **by Woongju Mun, M.S., S.M. ASCE<sup>1</sup> and John S. McCartney, Ph.D., P.E., M. ASCE<sup>2</sup>**

3            The isotropic compression response of compacted, low-plasticity clay specimens having  
4 various initial degrees of saturation  $S_{r,0}$  to high stresses under drained and undrained conditions  
5 was investigated using the approach of Mun and McCartney (2015). The compression curves in  
6 terms of void ratio  $e$  versus mean effective stress  $p'$  or mean total stress  $p$  are shown in Figure 1.

## 7            **DRAINED COMPRESSION RESPONSE**

8            After an initial elastic response, the drained specimens reach an apparent mean effective  
9 preconsolidation stress that increases with decreasing  $S_{r,0}$ . As  $p'$  increases further, the compression  
10 curves for the unsaturated specimens converge with the curve for the saturated specimen as air is  
11 expelled. The value of  $p'$  required to reach the point of pressurized saturation increases with  
12 decreasing  $S_{r,0}$ . At higher  $p'$ , the initial soil structure induced by compaction has an effect on the  
13 shape of the compression curves, which are also distorted by the use of the logarithmic scale.

## 14            **UNDRAINED COMPRESSION RESPONSE**

15            The compression curves for undrained specimens with a lower  $S_{r,0}$  have a softer response due  
16 to the compression of the air-filled voids. With increasing mean total stress, the pore air dissolves  
17 into the pore water until reaching the point of pressurized saturation, which depends on  $S_{r,0}$ . After  
18 this point, the specimens are water-saturated and the shapes of the compression curves are  
19 dominated by the pore water compressibility. The point of pressurized saturation can be assessed  
20 by revisiting the model of Hilf (1948), who combined Boyle's law and a simplified version of  
21 Henry's law to estimate changes in pore air pressure during undrained compression. Specifically,

---

<sup>1</sup> Research Associate, Department of Structural Engineering, University of California San Diego, CA 92093, USA.  
E-mail: musim21@gmail.com

<sup>2</sup> Associate Professor, University of California San Diego, Department of Structural Engineering, 9500 Gilman Dr.,  
La Jolla, CA 92093-0085, mccartney@ucsd.edu.

22 by considering a pressure-dependent solubility of air in water ( $h=u_a/k_h$ , where  $u_a$  is the pore air  
 23 pressure and  $k_h$  is Henry's constant), the value of  $\Delta u_a$  for a change in mean total stress  $\Delta p$  can be  
 24 calculated, as follows:

$$25 \quad \left( \frac{S_{r,0}n_0}{k_h} \right) \Delta u_a^2 + \left( (1 - S_{r,0})n_0 + \frac{2u_{a0}S_{r,0}n_0}{k_h} - m_{v,u} \Delta p \right) \Delta u_a - m_{v,u}u_{a0}\Delta p = 0 \quad (1)$$

26 where  $n_0$  is the initial porosity,  $u_{a0}$  equals 101.3 kPa, and  $m_{v,u}$  is the coefficient of volume  
 27 compressibility of the soil in undrained conditions. The change in mean total stress required to  
 28 reach pressurized saturation ( $\Delta p_{ps}$ ) can then be estimated as follows:

$$29 \quad \Delta p_{ps} = \frac{(1 - S_{r,0})n_0\Delta u_{a,ps} + \frac{S_{r,0}n_0}{k_h}(\Delta u_{a,ps}^2 + 2\Delta u_{a,ps}u_{a0})}{m_{v,u}(\Delta u_{a,ps} + u_{a0})} \quad (2)$$

30 The predicted values of  $\Delta p_{ps}$  for specimens having different values of  $S_{r,0}$  is shown in Figure 2  
 31 along with the experimental points of pressurized saturation from the undrained compression  
 32 curves in Figure 1. A good match is observed, with differences due to the choice of  $m_{v,u}$  for  
 33 specimens with different  $S_{r,0}$  values.

## 34 **IMPLICATIONS**

35 Although the trends in preconsolidation stress for the drained curves are well-captured by  
 36 available suction-hardening models, the process of pressurized saturation and the slope of the  
 37 compression curve for unsaturated soils need to be better characterized. The shapes of the drained  
 38 curves at high  $p'$  indicate that a bi-log-linear compression curve should not be used for values of  
 39  $p'$  greater than 10 MPa. Instead, an exponential decay model may better capture the transition to  
 40 void closure. The transition point at which the undrained compression curve is dominated by the  
 41 air-filled voids or the water-filled voids can be better captured using the modified analysis of Hilf  
 42 (1948).

43 **ACKNOWLEDGEMENTS**

44 Funding from ONR grant N00014-11-1-0691 is acknowledged.

45 **REFERENCES**

46 Hilf, J.W. (1948). "Estimating construction pore pressures in rolled earth dams." Proc. 2nd Int.

47 Conf. on Soil Mechanics and Foundation Engineering. Rotterdam, Vol. 3, 230-240.

48 Mun, W., and McCartney, J.S. (2015). "Compression mechanisms of unsaturated clay under high

49 stress levels." Can. Geot. J. 52(12), 2099-2112.

50 **LIST OF FIGURE CAPTIONS**

51 **Fig. 1.** Compression curves of compacted clay specimens having different  $S_{r,0}$  measured under

52 drained and undrained conditions

53 **Fig. 2.** Mean total stresses required to reach pressurized saturation for undrained, compacted clay

54 specimens having different  $S_{r,0}$

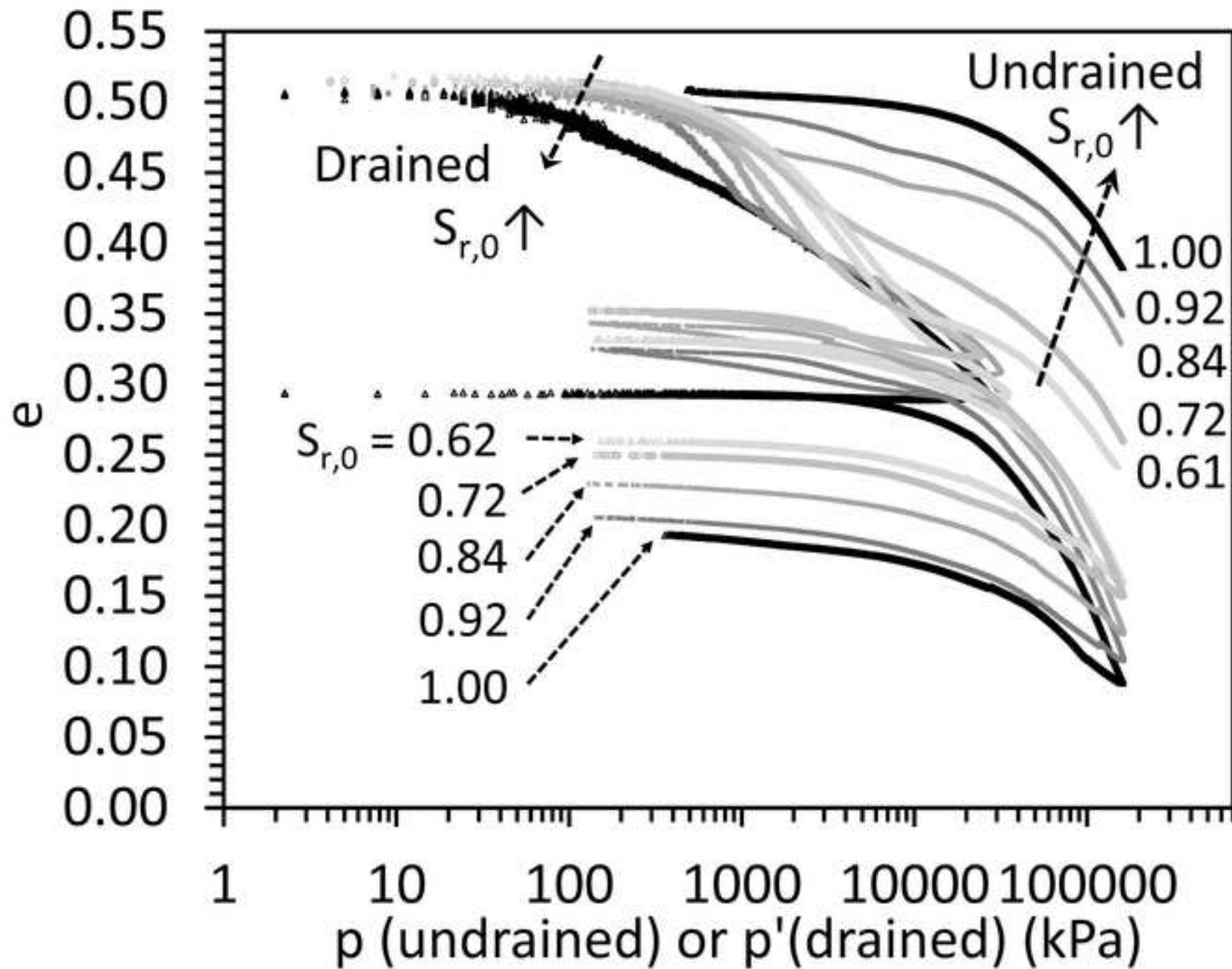


Figure 2

